J. Cent. South Univ. (2016) 23: 317−323
DOI: 10.1007/s11771-016-3076-2

Springer

Single-step synthesis of magnetic chitosan composites and application for chromate (Cr(VI)) removal

YANG Wei-chun(杨卫春)[1, 2], TANG Qiong-zhi(唐琼芝)[1], DONG Shu-yu(董舒宇)[1],
CHAI Li-yuan(柴立元)[1, 2], WANG Hai-ying(王海鹰)[1, 2]

1. School of Metallurgy and Environment, Central South University, Changsha 410017, China;
2. Chinese National Engineering Research Center for Control & Treatment of Heavy Metal Pollution, Changsha 410017, China

Abstract: Magnetic chitosan composites (Fe_3O_4@chitosan) were synthesized in one single-step, characterized and applied in Cr(VI) removal from water. With the increase of loading proportion of chitosan, Cr(VI) adsorption capacity of Fe_3O_4@chitosan composites increased from 10.771 to 21.040 mg/g. The optimum adsorption capacities of Cr(VI) on Fe_3O_4@chitosan-3 were found in a pH range of 3.0−5.0. Kinetic study results show that the adsorption process follows pseudo-second-order model, indicating that the rate-limiting step in the adsorption of Cr(VI) involves chemisorptions. Moreover, FT-IR spectra analysis confirms that the amine and hydroxyl groups of chitosan are predominantly responsible for binding. Results from this work demonstrate that the prepared Fe_3O_4@chitosan composites possess great potential in Cr(VI) removal from contaminated water.

Key words: Cr(VI); magnetic chitosan; one single-step synthesis; adsorption

1 Introduction

Water contamination of chromium has become a serious pollution issue as it poses a threat to the environment and ecological health. The United States Environmental Protection Agency (EPA) set the maximum concentration limit (MCL) for chromium in drinking water of 0.1 mg/L [1] and the World Health Organization set a stricter threshold of 0.05 mg/L [2]. The most common forms of chromium are hexavalent chromium (Cr(VI) and trivalent chromium (Cr(Ⅲ)). Cr(VI) is highly soluble in aqueous media, acutely toxic, mutagenic, and carcinogenic [3]. Thus, the removal of Cr(VI) from natural waters has attracted considerable attention. Typical methods used for Cr(VI) removal from water include precipitation, reduction, electrolytic removal, ion exchange, reverse osmosis, and adsorption [4−7]. Adsorption has been considered one of the most promising technologies for Cr(VI) removal in terms of cost, simplicity of design and operation [8−9]. A wide range of adsorbents, such as carbonaceous material (biocharc [10], active carbon [11]), metal oxides [9, 12−13], kaolin clay [14], have been reported for Cr(VI) removal. However, there were several problems associated with their use, such as low adsorption efficiency, poor mechanical strength.

Chitosan is not only inexpensive and abundant in nature, but it also has been recognized as a potential bioadsorbent for the removal of metals ions since its hydroxyl and amino groups can act as coordination sites for metal ions [15]. Even though advanced results have been obtained, it can be difficult to separate chitosan-based adsorbents from the aqueous solution using traditional separation methods such as filtration and sedimentation [16]. Magnetic materials have a high potential to be applied in adsorption systems because they can easily be separated in magnetic field. Iron oxide-based materials are the commonly applied magnetic particles because of their high magnetization and other favorable characteristics in terms of cost, environmental impact and chemical stability (e.g. resistance to acids and bases, low solubility) [17−18]. In order to benefit from the advantages of both of these two kinds of adsorbents, a magnetic chitosan composite adsorbent was developed [16, 19−22]. However, there are few studies on application of magnetic chitosan for Cr(VI) removal, and the synthesis procedure for the magnetic chitosan composite is typically accomplished in two or three steps. The first step often involves the preparation of magnetic materials and the second step involves the coating or dispersion of the magnetic

Foundation item: Projects(51304252, 51374237) supported by the National Natural Science Foundation of China
Received date: 2014−12−15; **Accepted date:** 2015−05−20
Corresponding author: WANG Hai-ying, Associate Professor; Tel: +86−731−88830875; E-mail: haiyw25@163.com

materials with chitosan [16]. The synthesis procedures for the modification of chitosan should be simplified. The preparation of MCCs in a single step should be encouraged.

In this work, a magnetic chitosan composite adsorbent for Cr(VI) removal was synthesized in one-single step via in situ synthetic route and characterized. The adsorption behavior and mechanism of Cr(VI) on magnetic chitosan composite was investigated.

2 Materials and methods

2.1 Materials

All chemicals were of analytical reagent grade. Ferric chloride ($FeCl_3·6H_2O$), ferrous chloride ($FeCl_2·4H_2O$), chitosan and potassium dichromate were purchased from Sinopharm Chemical Reagent Co., Ltd. (Shanghai, China). The molecular mass of chitosan, provided by the manufacturer, was 100 kg/mol.

The Cr(VI) stock solution(100 mg(Cr)/L) was prepared by dissolving proper amount of potassium dichromate in distilled water. Experimental solutions for adsorption and analysis were freshly prepared by diluting Cr(VI) stock solution with distilled water.

2.2 Preparation of bare Fe_3O_4 and chitosan-coated magnetite

The preparation of chitosan-coated magnetite in this study was prepared as follows. Different amounts of chitosan of 0, 1.78, 3.57, 10.71 and 14.28 g were dissolved in 150 mL of 10%−15% (v/v) acetic acid solution, stir it well until dissolved. Then, 8.39 g of $FeCl_3·6H_2O$ and 3.08 g $FeCl_2·4H_2O$ were dissolved into the above solution (the amount of Fe_3O_4 prepared was assumed to be 3.57 g). Afterwards, the resulting solution was added dropwise into 600 mL of 30%(v/v) NaOH solution over a period of 1 h under vigorous stirring. Then the suspension was left undisturbed for 4 h and then washed with deionized water several times and dried at 60 °C for 24 h to obtain the adsorbent (Fe_3O_4@chitosan). The adsorbents of Fe_3O_4@chitosan with initial mass ratios of Fe_3O_4 to chitosan varied as 1:0, 1:0.5, 1:1, 1:3 and 1:4 were denoted as Fe_3O_4, Fe_3O_4@chitosan-0.5, Fe_3O_4@chitosan-1, Fe_3O_4@chitosan-3 and Fe_3O_4@chitosan-4, respectively.

2.3 Characterization

The morphology of the Fe_3O_4@chitosan was characterized by scanning electron microscopy (SEM, JSM-6360). The X-ray diffraction (XRD) patterns of the Fe_3O_4@chitosan were obtained using Rigaku D/Max-RB diffractometer with Cu K_α radiation (λ=0.15406 nm, 35 kV, 40 mA). The magnetic properties of the adsorbents were measured with a vibrating sample magnetometer (VSM, HH-15, Nanjing University Instrument Plant, China) at room temperature. Specific surface area of chitosan-coated magnetite was measured by adsorption−desorption of ultrapure N_2 on a quantachrome instruments system (Adsorb SI) via Brunauer−Emmett−Teller (BET) method. Fourier transformed infrared spectroscopy (FT-IR) spectra of the product was obtained using a Nicolet IS10 spectrometer (Thermo Fisher, USA) at 4 cm^{-1} resolution.

2.4 Adsorption experiments

All the adsorption experiments were performed in 120 mL polyethylene vials filled with 100 mL aqueous Cr(VI) solution and 0.1 g adsorbent, and the vials were placed in thermostatic water bath and shaken for 24 h at 25 °C, afterwards, the samples were filtered using a 0.45-μm membrane filter (Millipore, Billerica, MA, USA) and the Cr(VI) concentration in solutions was determined by visible spectrophotometer (722 s, Shanghai Precision Science Instrument, Ltd.) using 1,5-diphenylcarbazide method[23]. While selected samples were used to determine the total chromium by potassium permanganate oxidation-diphenylcarbazide spectrophotometric [24]. The Cr(VI) concentration in solution was very closed to total chromium in solution. The amount of Cr(VI) adsorbed was calculated from the measured aqueous concentration based on mass balance. Meanwhile, blanks were analyzed to determine losses to reactor material and show minimal effect.

The adsorption isotherm was studied by varying initial Cr(VI) concentration from 2 to 45 mg/L at pH 4.0±0.1. Kinetic experiments were carried out at pH 4.0 with two initial Cr(VI) concentrations (2.13 and 9.81 mg/L), and at selected time intervals, samples were withdrawn and analyzed for residual Cr(VI) concentration. The effects of pH on Cr(VI) adsorption were investigated by adjusting initial solution pH from 3.0 to 9.0 using 0.1 mol/L HCl and 0.1 mol/L NaOH with initial Cr(VI) concentration of 10 mg/L. All the experimental data were the average of triplicate determinations with relative errors under 5%.

3 Results and discussion

3.1 Effect of Fe_3O_4 to chitosan mass ratio on Cr(VI) adsorption

To determine the optimal mass ratio of Fe_3O_4 to chitosan, a series of Fe_3O_4@chitosan composites with different mass ratios of Fe_3O_4 to chitosan from 1:0 to 1:4, were synthesized and tested for magnetic property and Cr(VI) adsorption. The saturation magnetization of

Fe_3O_4, Fe_3O_4@chitosan-0.5, Fe_3O_4@chitosan-1, Fe_3O_4@chitosan-3 and Fe_3O_4@chitosan-4 were 47.64, 32.33, 27.13, 19.44 and 15.33 A·m^2/kg, respectively. It is suggested that the coating of chitosan leads to a decrease in the magnetic properties of the composite. MA et al [25] found that a saturation value of 16.3 A·m^2/kg was sufficient for magnetic separation. Thus, the saturation magnetization value achieved with Fe_3O_4@chitosan-3 was high enough for magnetic separation.

Figure 1 shows the adsorption isotherms of Cr(VI) on Fe_3O_4@chitosan composites with various mass ratio of Fe_3O_4 to chitosan. It is suggested that Cr(VI) adsorption increases obviously with an increasing mass ratio of chitosan. When the mass ratio of Fe_3O_4 to chitosan reached 1:3, the adsorption amount of Cr(VI) did not change significantly.

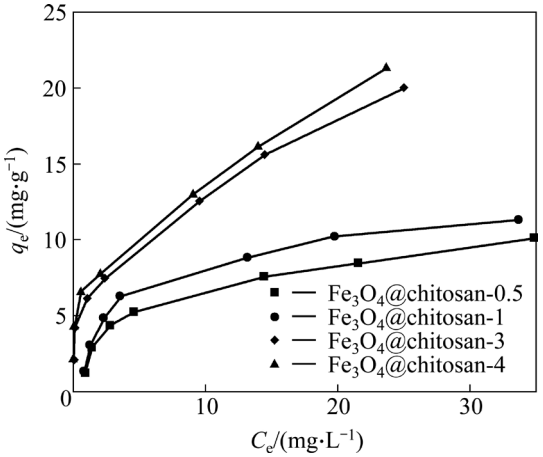

Fig. 1 Adsorption isotherms of Cr(VI) on Fe_3O_4@chitosan composites with various of mass ration of Fe_3O_4 to chitosan

The isotherm models of Langmuir and Freundlich were used to fit the experimental adsorption equilibrium data of Cr(VI) on magnetic adsorbents. The Langmuir model and Freundlich model are represented as Eqs. (1) and (2), respectively.

$$q_e = \frac{q_{max} b C_e}{1 + b C_e} \quad (1)$$

$$q_e = K_F C_e^n \quad (2)$$

where q_e(mg/g) is the amount of Cr(VI) adsorbed per unit mass of adsorbent; C_e(mg/L) is the mass concentration of Cr(VI) at equilibrium; b is the equilibrium adsorption constant related to the affinity of binding sites (L/mg); q_{max} is the maximum amount of the arsenic per unit mass of adsorbent; K_F is roughly an indicator of the adsorption capacity; n is the heterogeneity factor which has a lower value for more heterogeneous surfaces. The adsorption parameters obtained from the isotherms are presented in Table 1. As listed in Table 1, higher regression coefficient suggests that the Freundlich model is more suitable for describing the adsorption behavior of Cr(VI) on Fe_3O_4@chitosan composites. The Langmuir model assumes that adsorption occurs on a homogeneous surface. A heterogeneous surface of the Fe_3O_4@chitosan composites may be formed because of the simultaneous presence of chitosan and iron oxide in the composite. The calculated Cr(VI) adsorption capacity of Fe_3O_4@chitosan by Langmuir model increases from 10.771 to 21.040 mg/g as the coating of chitosan increases. The Freundlich model describes sorption where the sorbent has a heterogeneous surface with sorption sites that have different sorption energies. Fe_3O_4@chitosan-0.5 to Fe_3O_4@chitosan-4 for Cr(VI) adsorption exhibit decreased n value, indicating that the adsorption process becomes easier and more efficient [26].

Considering comprehensively adsorption effectiveness and magnetic property, the Fe_3O_4@chitosan-3 composites was chosen as feasible sorbent and was detailed examined in the following sections.

Table 1 Freundlich and Langmuir model parameters for Cr(VI) adsorption

Adsorbent	Freundlich model			Langmuir model		
	K_F	n	R^2	q_{max}	b	R^2
Fe_3O_4@chitosan-0.5	2.547	0.394	0.976	10.771	0.207	0.977
Fe_3O_4@chitosan-1	3.161	0.379	0.970	12.301	0.248	0.982
Fe_3O_4@chitosan-3	6.059	0.357	0.979	20.939	0.246	0.878
Fe_3O_4@chitosan-4	6.898	0.334	0.970	21.040	0.317	0.843

3.2 Characterizations of Fe_3O_4@chitosan-3

The specific surface area of Fe_3O_4@chitosan-3 was determined to be 62.5 m^2/g. The SEM images of Fe_3O_4@chitosan-3 and Fe_3O_4 are shown in Fig. 2. It is indicated that that the surface morphology of Fe_3O_4@chitosan-3 (Fig. 2(a)) appeared to have a fluffy and irregular porous texture. The XRD pattern (Fig. 3(a)) of the Fe_3O_4@chitosan-3 proved that in the composite, the main peaks at 2θ=30.4°, 35.6°, 43.3°, 57.3°, and 62.8° are characteristic peaks of Fe_3O_4. FT-IR spectra of the Fe_3O_4@chitosan-3 (Fig. 3(b)) shows that the characteristic absorption bands for chitosan appear at 3420 cm^{-1} (O—H and N—H stretching vibrations), 1620^{-1} (N—H bending vibrations) and 1069 cm^{-1} (—C—OH stretching vibrations).

SEM, XRD and FT-IR results are important because they proved the successful coating of magnetite by chitosan with the aid of NaOH. Chitosan on the surface is available for coordinating with Cr(VI) ions. The synthetic procedure of Fe_3O_4@magnetite composites is schematically presented in Fig. 4.

3.3 Effect of initial pH value

The Cr(VI) adsorption behavior on Fe_3O_4@chitosan-3 is pH-dependent. The effect of pH on

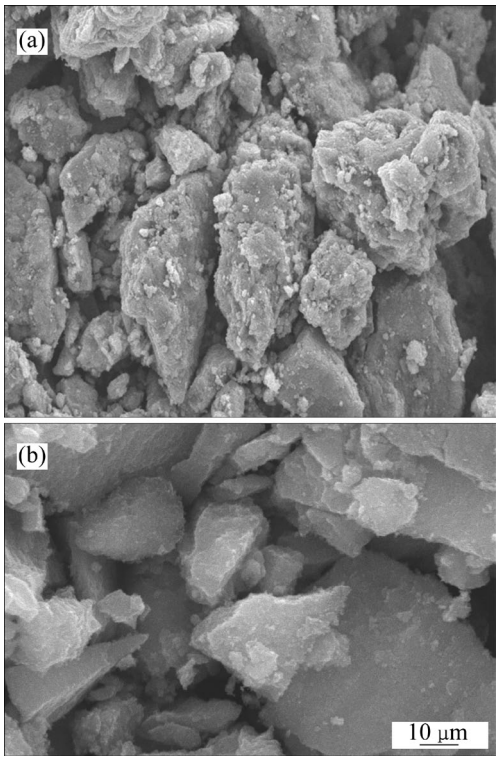

Fig. 2 SEM images of Fe_3O_4@chitosan-3 (a) and Fe_3O_4(b)

the adsorption of Cr(VI) onto Fe_3O_4@chitosan-3 is shown in Fig. 5. The maximum adsorption is obtained at pH 3.0; the removal efficiency is almost 100%. The adsorption of Cr(VI) decreases with increasing pH. A strong pH-dependence is observed for Cr(VI) removal by the Fe_3O_4@chitosan-3, suggesting that adsorption or binding is mainly controlled by electrostatic interactions. Whereas at a lower pH solution the number of positively charged active sites increased due to the protonation of functional groups of Fe_3O_4@chitosan-3 composite, and Cr(VI) was mainly in the form of anion; this increases the electrostatic attraction between the negatively charged anions and positively charged surface of Fe_3O_4@chitosan-3 composite, resulting in an increase in anionic Cr(VI) adsorption. The optimum adsorption capacities of Cr(VI) were found in a pH range of 3.0−5.0.

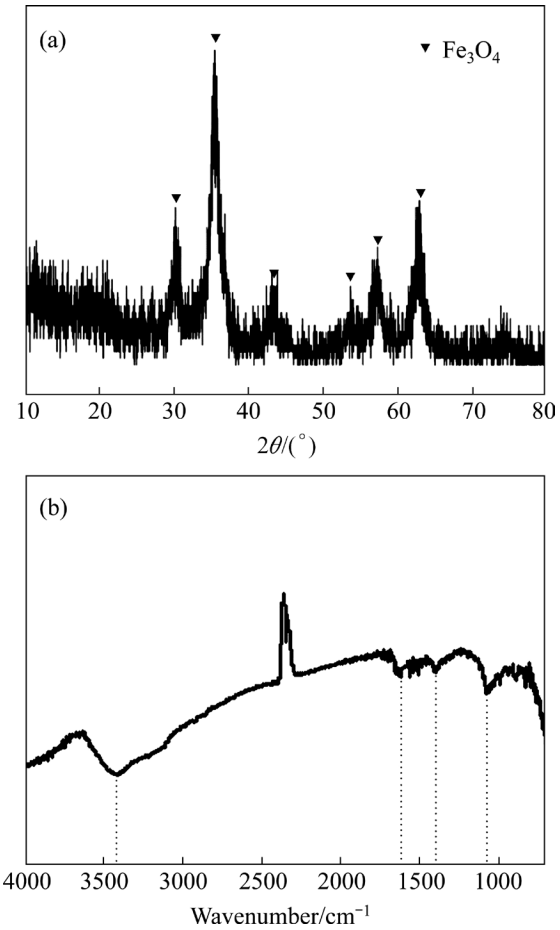

Fig. 3 XRD pattern (a) and FT-IR spectra (b) of Fe_3O_4@chitosan-3

3.4 Adsorption kinetics

Figure 6 shows the time-dependence of Cr(VI) adsorption on the Fe_3O_4-chitosan-3 composites adsorbent at various initial concentrations. The process was obviously time-dependent, and the adsorption was rapid in the first 60 min (nearly 90% removal of Cr(VI) can be achieved), and thereafter it proceeded at a relatively slow rate.

The pseudo-first-order, pseudo-second-order and Elovich kinetic models were applied to describing the kinetics of Cr(VI) adsorption on the composite. The fits

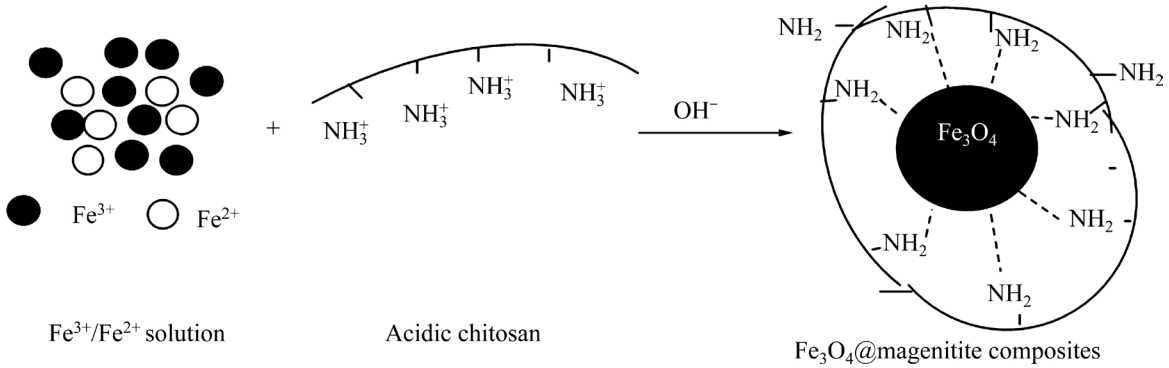

Fig. 4 Schematic formation process of Fe_3O_4@magenitite composites

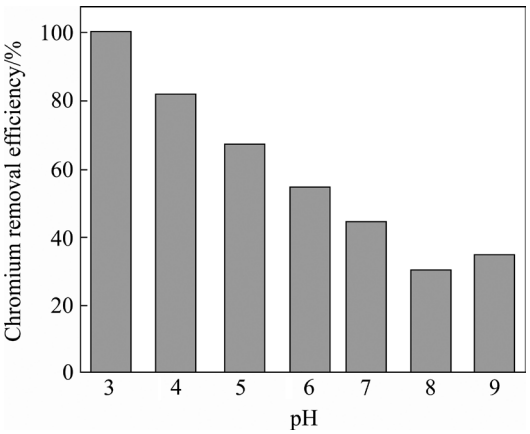

Fig. 5 Effect of pH on chromium removal efficiency

of the three kinetic models to the Cr(VI) adsorption kinetic data are shown in Figs. 6(b), (c) and (d), and the model parameters obtained by curve-fitting kinetic data are listed in Table 2. Pseudo-second-order model was considered more suitable in describing the adsorption kinetics of Cr(VI) on the adsorbent according to the related coefficient (R^2) (Table 2). Pseudo-second-order model considers chemisorption process. This is an indication that the rate-limiting step in the adsorption of Cr(VI) onto Fe_3O_4-chitosan-3 composites adsorbent involves chemisorptions due to valence forces through the sharing or exchange of electrons between sorbent and sorbate, complexation, coordination, and/or chelation [27].

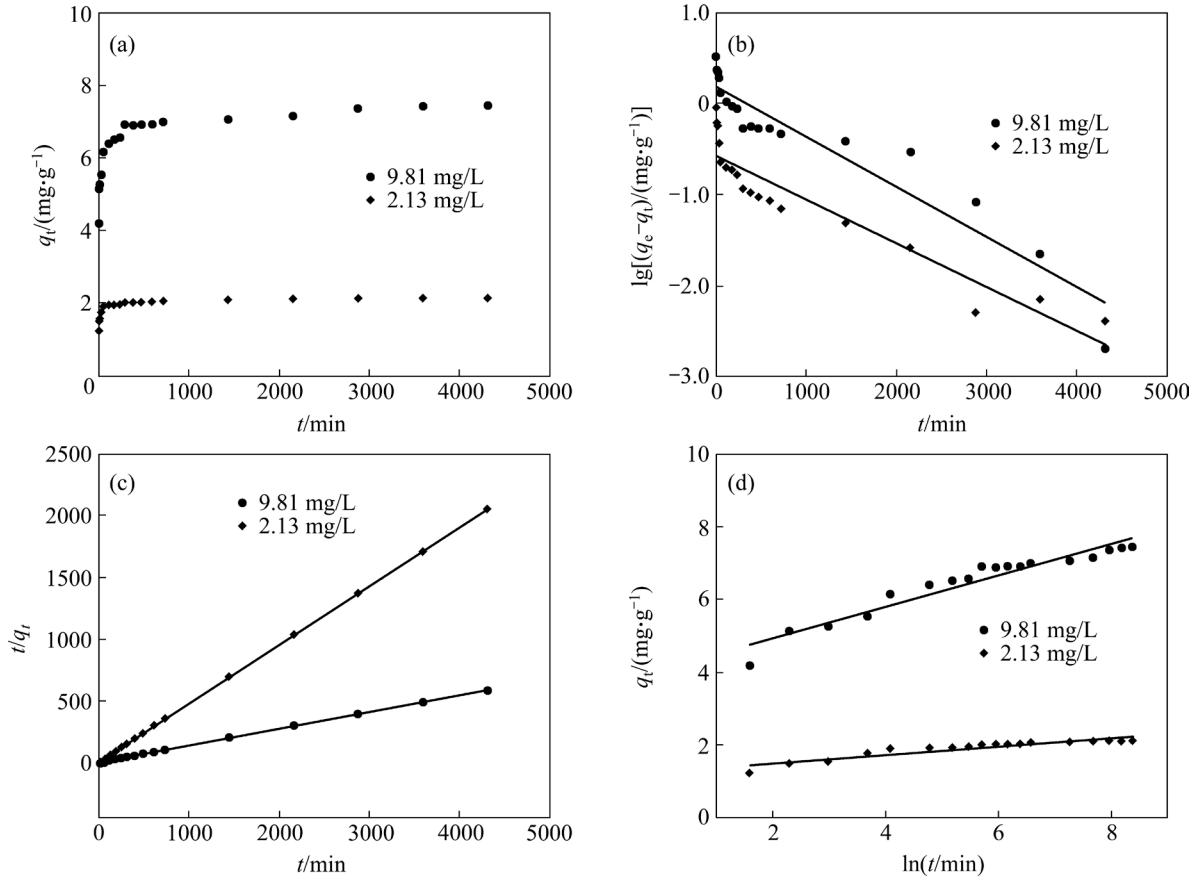

Fig. 6 Effect of reaction time on Cr(VI) adsorption: (a) Kinetics modeling of Cr(VI) adsorption; (b) Pseudo-first-order kinetic plots; (c) Pseudo-second-order kinetic plots; (d) Elovich model plots (t is the reaction time; q_e (mg/g) and q_t (mg/g) are the amounts of adsorbed Cr(VI) at equilibrium and at any reaction time t)

Table 2 Kinetic and statistical parameters of three kinetic models

C_e/(mg·L^{-1})	Pseudo-first-order model: $\lg(q_e-q_t)=\lg q_e-\frac{k_1}{2.303}t$			Pseudo-second-order model: $\frac{t}{q_t}=\frac{1}{k_2q_e^2}+\frac{1}{q_e}t$			Elovich model: $q_t=\beta\ln(\alpha\beta)+\beta\ln t$		
	q_e	k_1	R^2	q_e	k_2	R^2	α	β	R^2
9.81	1.551	1.38×10^{-3}	0.899	7.418	4.98×10^{-3}	0.999	6.31×10^{3}	0.430	0.927
2.13	0.267	1.15×10^{-3}	0.875	2.115	3.07×10^{-2}	1.000	1.18×10^{4}	0.113	0.857

Note: t is the reaction time (min); q_e(mg/g) and q_t(mg/g) are the amounts of adsorbed Cr(VI) at equilibrium and at any reaction time t; k_1(min) and k_2 (g·min/mg) are the equilibrium rate constants for pseudo-first-order and pseudo-second-order models respectively; Elovich constant α is related to the sorption rate while β is related to the surface coverage; R^2 is correlation coefficient.

3.5 FT-IR spectra analysis

The function groups and surface chemical properties are of importance to understand the adsorption mechanism of Cr(VI) onto the composites.

To confirm the adsorption mechanism of Cr(VI) onto Fe_3O_4@chitosan-3, the changes characteristic adsorption bands in the adsorbent before and after adsorption were investigated by FT-IR (Fig. 7). A slight shift from 3420 to 3400 cm^{-1} occurs following chromium adsorption, suggesting an enhanced hydrogen bond. The relative intensities of N—H bending vibration bands (1620 cm^{-1}) and —C—OH stretching vibration bands (1069 cm^{-1}) increased, which provides an evidence for possible protonation reaction on amine and hydroxyl groups. It is suggested that the amine and hydroxyl groups of chitosan are predominantly responsible for binding. However, more studies and further evidence are needed to fully understand the adsorption mechanism of Cr(VI) onto the composites.

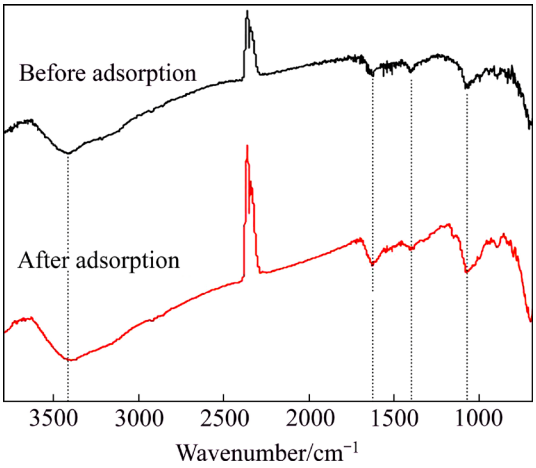

Fig. 7 FT-IR spectra of Fe_3O_4@chitosan-3 before and after chromium adsorption

4 Conclusions

1) The magnetic chitosan composites (Fe_3O_4@chitosan) can be synthesized in one single-step. The calculated Cr(VI) adsorption capacity of Fe_3O_4@chitosan by Langmuir model increases from 10.771 to 21.040 mg/g as the coating of chitosan increases.

2) The optimum adsorption capacities of Cr(VI) on Fe_3O_4@chitosan-3 are found in a pH range of 3.0−5.0. Kinetic study result of Cr(VI) adsorption on Fe_3O_4@chitosan-3 shows that the adsorption process followed pseudo-second-order model, indicating the rate-limiting step in the adsorption of Cr(VI) involves chemisorptions.

3) FT-IR spectra analysis confirms that the amine and hydroxyl groups of chitosan are predominantly responsible for binding. Results demonstrate the prepared Fe_3O_4@chitosan composites possess potential in Cr(VI) contaminated water.

References

[1] US EPA. National primary drinking water regulations [S]. [2006−01−23] http://water.epa.gov/drink/contaminants/index.cfm#List.

[2] WHO. Chromium in drinking-water. Background document for preparation of WHO Guidelines for drinking-water quality [R]. World Health Organization: Geneva (WHO/SDE/WSH/03.04/4), 2003.

[3] JIANG Wen-jun, CAI Quan, XU Wei, YANG Ming-wei, CAI Yong, DIONYSIOU D D, O'SHEA K E. Cr(VI) Adsorption and reduction by humic acid coated on magnetite [J]. Environment Science and Technology, 2014, 48: 8078−8085.

[4] ARAVINDHAN R, MADHAN B, RAO J R, NAIR B U, RAMASAMI T. Bioaccumulation of chromium from tannery wastewater: An approach for chrome recovery and reuse [J]. Environment Science and Technology, 2004, 38: 300−306.

[5] RENGARAJ S, JOO C K, KIM Y, YI J. Kinetics of removal of chromium from water and electronic process wastewater by ion exchange resins: 1200H, 1500H and IRN97H [J]. Journal of Hazardous Material, 2003, 102: 257−275.

[6] HAFEZA A, EL-MARIHARAWY S. Design and performance of the two-stage/two-pass RO membrane system for chromium removal from tannery wastewater. Part 3 [J]. Desalination, 2004, 165: 141−151.

[7] HAO Tao, YANG Chao, RAO Xue-hui, WANG Ji-de, NIU Chun-ge, SU Xin-tai. Facile additive-free synthesis of iron oxide nanoparticles for efficient adsorptive removal of Congo red and Cr(VI) [J]. Applied Surface Science, 2014, 292: 174−180.

[8] DEVECI H, KAR Y. Adsorption of hexavalent chromium from aqueous solutions by bio-chars obtained during biomass pyrolysis [J]. Journal of Industrial and Engineering Chemistry, 2013, 19(1): 190−196.

[9] QUSTI A H. Removal of chromium (VI) from aqueous solution using manganese oxide nanofibers [J]. Journal of Industrial and Engineering Chemistry, 2014, 20: 3394−3399.

[10] AGRAFIOTI E, KALDERIS D, DIAMADOPOULOS E. Arsenic and chromium removal from water using biochars derived from rice husk, organic solid wastes and sewage sludge [J]. Journal of Environmental Management, 2014, 133: 309−314.

[11] SANDHYA B, TONNI A K. Cr(VI) removal from synthetic wastewater using coconutshell charcoal and commercial activated carbon modified with oxidizing agents and/or chitosan [J]. Chemosphere, 2004, 54: 951−967.

[12] JOHNSTON C P, CHRYSOCHOOU M. Mechanisms of chromate adsorption on hematite [J]. Geochimica et Cosmochimica Acta, 2014, 138: 146−157.

[13] JIA Zhi-gang, WANG Qiu-ze, REN Da-ping, ZHU Rong-sun. Fabrication of one-dimensional mesoporous α-Fe_2O_3 nanostructure via self-sacrificial template and its enhanced Cr(VI) adsorption capacity [J]. Applied Surface Science, 2013, 264(1): 255−260.

[14] DENG Lin, SHI Zhou, LUO Lu, CHEN Shi-yang, YANG Ling-fang, YANG Xiu-zhen, LIU Li-shan. Adsorption of hexavalent chromium onto kaolin clay based adsorbent [J]. Journal of Central South University, 2014, 21(10): 3918−3926.

[15] VIEIRA R S, MENEGHETTI E, BARONI P, GUIBAL E, de la CRUZ V M, CABALLERO A, RODRíGUEZ-CASTELLÓN E, BEPPU M M. Chromium removal on chitosan-based sorbents—An EXAFS/XANES investigation of mechanism [J]. Materials Chemistry and Physics, 2014, 146: 412−417.

[16] KUMAR REDDY D H, LEE S M. Application of magnetic chitosan composites for the removal of toxic metal and dyes from aqueous solutions [J]. Advances in Colloid and Interface Science, 2013, 201/202: 68−93.

[17] WANG Jia-hong, ZHENG Shou-rong, SHAO Yun, LIU Jing-liang, XU Zhao-yi, ZHU Dong-qing. Amino-functionalized Fe_3O_4@SiO_2 core–shell magnetic nanomaterial as a novel adsorbent for aqueous heavy metals removal [J]. Journal of Colloid and Interface Science, 2010, 349: 293−299.

[18] CHAI Li-yuan, WANG Yun-yan, ZHAO Na, YANG Wei-chun, YOU Xiang-yu. Sulfate-doped Fe_3O_4/Al_2O_3 nanoparticles as a novel adsorbent for fluoride removal from drinking water [J]. Water Research, 2013, 47(12): 4040−4049.

[19] TRAN H V, TRAN L D, NGUYEN T N. Preparation of chitosan/magnetite composite beads and their application for removal of Pb(II) and Ni(II) from aqueous solution [J]. Materials Science and Engineering C, 2010, 30: 304−310.

[20] MONIER M, AYAD D M, WEI Y, SARHAN A A. Adsorption of Cu(II), Co(II), and Ni(II) ions by modified magnetic chitosan chelating resin [J]. Journal of Hazardous Material, 2010, 177: 962−970.

[21] HRITCU D, HUMELNICU D, DODI G, POPA M. Magnetic chitosan composite particles: evaluation of thorium and uranyl ion adsorption from aqueous solutions [J]. Carbohydrate Polymers, 2012, 87: 1185−1191.

[22] PODZUS P E, DEBANDI M V, DARAIO M E. Copper adsorption on magnetite-loaded chitosan microspheres: A kinetic and equilibrium study [J]. Physica B: Condensed Matter, 2012, 407(16): 3131−3133.

[23] DUPONT L, GUILLON E. Removal of hexavalent chromium with a lignocellulosic substrate extracted from wheat bran [J]. Environment Science and Technology, 2003, 37: 4235−4241.

[24] GB 7466−87. Water quality-Determination of total chromium [S]. 1987.

[25] MA Zhi-ya, GUAN Yue-ping, LIU Hui-zhou. Synthesis and characterization of micron-sized monodisperse superparamagnetic polymer particles with amino groups [J]. Journal of Polymer Science Part A-Polymer Chemistry, 2005, 43: 3433−3439.

[26] MOU F, GUAN J, MA H, XU L, SHI W. Magnetic iron oxide chestnutlike hierarchical nanostructures: Preparation and their excellent arsenic removal capabilities [J]. ACS Applied Materials and Interfaces, 2012, 4(8): 3987−3993.

[27] HO Y S, MCKAY G, WASE D A J, FORSTER C F. Study of the sorption of divalent metal ions on to peat [J]. Adsorption Science and Technology, 2000, 18: 639−650.

(Edited by YANG Hua)